Cooperative Interaction of Human XPA Stabilizes and Enhances Specific Binding of XPA to DNA Damage†

Yu Liu,‡ Yiyong Liu,‡ Zhengguan Yang,‡ Christopher Utzat,§ Guizhi Wang,‡ Ashis K. Basu,§ and Yue Zou*,‡

Department of Biochemistry and Molecular Biology, Quillen College of Medicine, East Tennessee State University, Johnson City, Tennessee 37614, and Department of Chemistry, University of Connecticut, Storrs, Connecticut 06269

Received November 13, 2004; Revised Manuscript Received February 23, 2005

ABSTRACT: Human xeroderma pigmentosum group A (XPA) is an essential protein for nucleotide excision repair (NER). We have previously reported that XPA forms a homodimer in the absence of DNA. However, what oligomeric forms of XPA are involved in DNA damage recognition and how the interaction occurs in terms of biochemical understanding remain unclear. Using the homogeneous XPA protein purified from baculovirus-infected sf21 insect cells and the methods of gel mobility shift assays, gel filtration chromatography, and UV-cross-linking, we demonstrated that both monomeric and dimeric XPA bound to the DNA adduct of *N*-acetyl-2-aminofluorene (AAF), while showing little affinity for nondamaged DNA. The binding occurred in a sequential and protein concentration-dependent manner. At relatively low-protein concentrations, XPA formed a complex with DNA adduct as a monomer, while at the higher concentrations, an XPA dimer was involved in the specific binding. Results from fluorescence spectroscopic and competitive binding analyses indicated that the specific binding of XPA to the adduct was significantly facilitated and stabilized by the presence of the second XPA in a positive cooperative manner. This cooperative binding exhibited a Hill coefficient of 1.9 and the step binding constants of $K_1 = 1.4 \times 10^6$ M^{-1} and $K_2 = 1.8 \times 10^7$ M^{-1}. When interaction of XPA and RPA with DNA was studied, even though binding of RPA−XPA complex to adducted DNA was observed, the presence of RPA had little effect on the overall binding efficiency. Our results suggest that the dominant form for XPA to efficiently bind to DNA damage is the XPA dimer. We hypothesized that the concentration-dependent formation of different types of XPA-damaged DNA complex may play a role in cellular regulation of XPA activity.

The human XPA (xeroderma pigmentosum group A) protein is an indispensable protein of human nucleotide excision repair (NER) that recognizes and removes a large variety of structurally distinct bulky DNA lesions (*1*−*3*). The XPA gene is required for both global genome repair (GGR) and transcription-coupled repair (TCR) (*4*, *5*). The protein with a zinc finger motif is capable of binding specifically to the damaged DNA in vitro. XPA interacts with the replication protein A (RPA) to form a protein−protein complex, and this complex formation is believed to be important for NER.

A better understanding of the mechanism of human NER, and specifically determination of the role of human XPA, is being actively pursued by research groups including ours. Earlier reports suggest that XPA is involved in the DNA damage recognition process of NER and also plays a role in the NER complex and nuclease assembly (*6*−*8*). In the case of damage recognition, it is now generally believed that in GGR, XPA−RPA complex acts as a DNA damage verifier following the initial damage recognition by the XPC-HR23B in a double-checking mechanism (*3*, *9*−*11*). However, a recent in vivo study indicated that XPA molecules freely mobilized in cells and that recruiting of RPA onto DNA lesions was independent of XPA (*12*). Analogous results have been reported in another study (*13*). In TCR, where the XPC-HR23B is not necessary, the RNA polymerase complex has been proposed to play a substituting role for initial damage identification. By contrast, XPA is believed to be involved in both the GGR and the TCR for DNA damage recognition, and its presence is required in the final excision complex. Even so, the exact role and molecular mechanism of XPA in human NER remains unclear. In addition, we recently reported that XPA forms homodimer under normal experimental conditions (*18*). An interesting question that remains to be addressed is whether the XPA binds to DNA substrate in dimer or what is the most efficient form of XPA binding to DNA damage.

Previously, human XPA has been purified as a protein consisting of two bands migrating closely (a doublet) as analyzed by SDS−PAGE (*14*, *15*). The heterogeneousness of XPA appeared to be related to the reduction status of the seven cysteines in human XPA, which is important for the potential formation of disulfide bonds within the protein (*21*). Formation or lack of the disulfide bonds may alter the activity of proteins. Thus, a homogeneous XPA may serve as the best form for the determination of the biochemical functions of XPA.

† This study was supported by NCI Grant CA86927 (to Y.Z.) and NIEHS Grants ES09127 and ES 00318 (to A.K.B.)

* Corresponding author: Yue Zou, East Tennessee State University, James H. Quillen College of Medicine, Department of Biochemistry and Molecular Biology, Johnson City, TN 37614. Phone: (423) 439-7179. Fax: (423) 439-8235. E-mail: zouy@etsu.edu.

‡ East Tennessee State University.

§ University of Connecticut.

10.1021/bi047598y CCC: $30.25
Published on Web 04/22/2005

In the present study, we characterized the oligomeric interactions of homogeneous human XPA protein with the 50-bp DNA substrate containing a single AAF−DNA adduct. Our results showed that two different types of XPA−DNA adduct complexes formed in a protein concentration-dependent manner, involving the monomer and dimer of XPA, respectively. For the complex formation of the dimeric XPA with DNA substrate, the two XPA molecules bind to the DNA adduct in a stepwise and positively cooperative manner. The cooperative interaction, which occurred with the stepwise binding constants of $K_1 = 1.4 \times 10^6\ M^{-1}$ and $K_2 = 1.8 \times 10^7\ M^{-1}$, resulted in a significant stabilization effect on the XPA binding to damaged DNA. These results suggested that the XPA dimer is probably the major form of the protein involved in the DNA damage recognition. Surprisingly, the presence of RPA showed little effects on the specific binding affinity of XPA.

MATERIALS AND METHODS

Human XPA Purification. As described previously (*17*, *18*), $[His]_6$-XPA was expressed in sf21 cells infected with recombinant baculovirus pBac-XPA (graciously provided by J. J. Turchi, Wright State University School of Medicine) (*17*). To 2 L of fresh cell pellet, 25 mL of the lysis buffer (50 mM Tris, pH 8.0, 100 mM NaCl, 0.1% Triton X-100, 10% glycerol, 10 mM β-mercaptoethanol, 0.5 mM $ZnCl_2$, 0.5 mM PMSF, and protease inhibitor cocktail) was added. The lysate was gently stirred and dissolved completely before being applied to the French Press at 4 °C. This was followed by a brief sonication (5 × 0.1 s pulses) on ice water. The lysate was then spun at 16 000*g* for 15 min at 4 °C. Imidazole (1 mM) was prepared and added to the supernatant before being loaded onto a 5 mL Ni−NTA column equilibrated with buffer A (50 mM Tris, pH 8.0, 100 mM NaCl, 0.01% Triton X-100, 10% glycerol, 10 mM β-mercaptoethanol, 0.5 mM $ZnCl_2$, 0.5 mM PMSF, and 1 mM imidazole). The supernatant was allowed to flow through the Ni−NTA column twice, followed by extensive alternate washes with buffers A and B (50 mM Tris, pH 8.0, 500 mM NaCl, 0.01% Triton X-100, 10% glycerol, 10 mM β-mercaptoethanol, 0.5 mM $ZnCl_2$, 0.5 mM PMSF, and 1 mM imidazole). Then the protein was eluted from the column with buffer A containing imidazole of concentration of 10−80 mM. The fractions were pooled and further purified by Sephacryl S-200 column (Amersham Biosciences) by following the manufacturer's instructions. The fractions were again pooled and dialyzed against the storage buffer C (50 mM, Tris, pH 8.0, 100 mM NaCl, 0.01% Triton X-100, 50% glycerol, 1 mM DTT, and 0.5 mM $ZnCl_2$). After concentration by Amicon concentrator, aliquots of $[His]_6$-XPA protein were stored at −80 °C. The concentration of the protein was determined by using a Bio-Rad protein assay kit.

Gel Mobility Shift Assays. The gel mobility shift assays were used to demonstrate that XPA was functionally binding to the DNA substrates containing a single C8-guanine AAF adduct. Construction of the substrates was described previously (*19*). XPA of varying concentrations (with or without RPA) were mixed with the 5′-terminally [^{32}P]-labeled substrate (typically 1−2 nM) in 20 μL of binding buffer (20 mM Hepes, pH 7.9, 75 mM KCl, 5 mM $MgCl_2$, 1 mM EDTA, 1 mM DTT, 5% glycerol, and 100 μg/mL BSA). For the 50-bp DNA substrate, the mixture was incubated at 30 °C for 20 min, and for the 11-bp DNA substrate, the mixture was incubated at 16 °C for 20 min. Two microliters of 80% (v/v) glycerol was added to the mixture after incubation, immediately loaded onto 3.5% native polyacrylamide gel in TBE running buffer, and electrophoresed for 2 h at 4 °C.

Gel Filtration Chromatograph and Liquid Scintillation. Superdex-200 HR column and AKTA purifier system (both from Amersham Pharmacia Biotech) were used to perform the gel filtration chromatograph. Various concentrations of XPA protein were incubated with 5′-[^{32}P]-labeled 50-bp DNA in 200 μL of binding buffer as described above. The mixtures were then injected into a 200 μL sample loading loop connected onto the injector, and the system was running at a flow rate of 0.5 mL/min at 4 °C. Fractions of 200 μL each were collected. A mixture of the molecular markers (ribonuclease A, 13.7 kDa; chymotrysinogen A, 25 kDa; ovalbumin, 43 kDa; albumin, 67 kDa; aldolase, 158 kDa; catalase, 232 kDa; ferritin, 440 kDa; and thyroglobulin, 669 kDa) was also gel-filtered through the column in the same manner. Aliquots of 150 μL out of each of the collected fractions were then mixed with 3 mL SafeGel and vortexed for the scintillation counting (ScintiSafe Econo 2).

UV-Cross-Linking Analysis. The XPA protein with indicated concentrations was incubated with or without terminally [^{32}P]-labeled AAF-50-bp substrate in 20 μL XPA binding buffer at 30 °C for 20 min. The reaction was then transferred into the cap of an Eppendorf tube and subjected to the UV irradiation (254 or 312 nm) at 14 J m^{-2} s^{-1} for 10 min. After irradiation, samples were spun down into the Eppendorf tube, denatured with SDS gel loading buffer at 90 °C, and separated on 8% SDS−PAGE. The gel was either scanned by phosphorimager for radioactivity or analyzed by Western blotting with monoclone anti-XPA antibody. The Precision Plus Dual Color protein standard from Bio-Rad was used to indicate the molecular weight of cross-link products.

Competition Experiment. XPA protein at given concentrations was mixed with 5′-[^{32}P]-labeled AAF-50-bp DNA and incubated at 30 °C for 20 min in DNA binding buffer. Then, the nonradioactive and nondamaged 50-bp substrate with concentrations as indicated was added and incubated at 30 °C for another 20 min. Samples were then loaded onto a 3.5% native gel and electrophoresed at 80 V in TBE buffer at 4 °C for 2 h. Alternatively, the protein was also incubated with both damaged and nondamaged DNA together under the same experimental conditions, and no different results were obtained.

Fluorescence Anisotropy Analysis. We employed fluorescence anisotropy to characterize the specific binding of XPA to the 5′ terminally labeled fluorescein AAF-50-bp substrate (5′F-AAF-50-bp) and determined the binding cooperativity. The anisotropy titrations were performed at 25 °C on a SPEX Fluorolog-3 fluorometer (Jobin Yvon Inc., NJ) with an automated polarizer. The excitation wavelength was set at 492 nm and emission wavelength at 520 nm with a 500 nm cutoff filter and a slit width at 14 nm for both excitation and emission beams for reliable signals. After sample equilibration, data points with integration time of 5 s and standard error of 0.5% were collected for each titration point. To eliminate the potential effects of background upon addition of the protein, XPA and the DNA substrates were

placed in the same binding buffer prior to the titration. All titrations were performed in a micro quartz cuvette (4 mm × 4 mm) of a minimum sample volume of 200 μL with a 2 mm × 2 mm stirring bar. Each addition of XPA was 0.5−1 μL, delivered by a 25 μL Hamilton syringe using a Hamilton repeating dispenser. The degree of binding cooperativity was determined by the Hill coefficient (n) derived from Hill plot (*20*): $\log(\theta)$ versus $\log(L)$, where L is the concentration of free XPA which was reasonably substituted with the total concentration of XPA in this case as the protein concentrations used in this study were in large excess over the substrate concentration. The θ is defined by the following equation:

$$\theta = Y/(1 - Y)$$

Y is the fractional saturation of the DNA, the number of bound DNA sites per total number of binding sites (Y varies from 0 to 1), which is corresponding to the fractional anisotropy of DNA saturated with XPA.

Data Fitting and Processing. The binding of XPA to the DNA adduct can be described by the following equilibria:

$$A + D \leftrightarrow DA \qquad K_1 = \frac{[DA]}{[A][D]} \tag{1}$$

$$DA + A \leftrightarrow DA_2 \qquad K_2 = \frac{[DA_2]}{[A][DA]} \tag{2}$$

where A and D stand for XPA protein and DNA, respectively.

The fluorescence anisotropy change is proportional to the concentrations of XPA−DNA and XPA_2−DNA and can be defined as

$$\Delta r = a([DA] + b[DA_2]) = a(K_1[A][D] + bK_2[DA][A]) \tag{3}$$

where the a represents the proportional constant for signal from XPA−DNA, while the b is the proportional constant for signal from XPA_2−DNA relative to a.

The total concentrations of XPA and DNA can be written as

$$[A]_o = [A] + [DA] + 2[DA_2] \tag{4}$$

$$[D]_o = [D] + [DA] + [DA_2] \tag{5}$$

Subtraction of eq 4 − 5

$$[DA] = [A] - [A]_o - 2[D] + 2[D]_o \tag{6}$$

$$[D] = \frac{[DA]}{K_1[A]} = \frac{[A] - [A]_o - 2[D] + 2[D]_o}{K_1[D]}$$

$$[D] = \frac{[A] - [A]_o + 2[D]_o}{2 + (K_1[A])} \tag{7}$$

From eq 6,

$$[DA] = \frac{K_1[A]([A] - [A]_o + 2[D]_o)}{2 + (K_1[A])} \tag{8}$$

Combining eq 7, 8, and 3,

$$\Delta r = \frac{a([A] - [A]_o + 2[D]_o)(K_1[A] + bK_1K_2[A]^2)}{2 + (K_1[A])} \tag{9}$$

To determine the equilibrium or free concentration of XPA at each titration point which was experimentally unknown, eq 1, 2, and 4 were combined so that,

$$[A]_o = [A] + (K_1[A])\frac{[A] - [A]_o + 2[D]_o}{2 + (K_1[A])} + 2K_2[A]\frac{K_1[A]([A] - [A]_o + 2[D]_o)}{2 + (K_1[A])}$$

Thus, the equilibrium concentration of XPA can be determined by

$$K_1K_2[A]^3 + (K_1 - (K_1K_2[A]_o) + 2K_1K_2[D]_o)[A]^2 + (1 - (K_1[A]_o) + K_1[D]_o)[A] - [A]_o = 0 \tag{10}$$

Equation 10 can be solved with K_1 and K_2 as constants for [A], which is a solution meeting the requirement of $0 \le [A] \le [A]_o$.

Therefore, the experimental data are best fitted with eq 9 and 10 for determination of K_1 and K_2 by the nonlinear least-squares method

$$Z = \sum_i [(\Delta r_{cal})_i - (\Delta r_{exp})_i]^2 = \min \tag{11}$$

where i represents each titration data point. The Δr_{cal} and Δr_{exp} denote the signal changes obtained from eq 9 and experiments, respectively. The entire data fitting and processing were carried out with a program written with Microsoft Excel.

RESULTS

Purification of XPA. The XPA protein overexpressed from baculovirus-infected insect cells was purified following the procedures as describe previously (*17*) with modifications featured by the use of 100 mM NaCl rather than the concentration of 500 mM through the purification. The 100 mM concentration of salt appeared to be more physiologically relevant. As shown in Figure 1A, the XPA fractions eluted from a Sephacryl S-200 column displayed a single band on the Coomassie Blue-stained 8% SDS−PAGE. By contrast, when the concentration of NaCl at 500 mM was used in the purification, the protein homogeneity was compromised, resulting in the appearance of the double bands on the gel (Figure 1B). The homogeneous and soluble form of XPA appeared to be the same as the form I of the heterogeneous XPA (Figure 1C). As previously suggested, the heterogeneousness of XPA was probably caused by the different reduction statuses of XPA and thus related to the formation of disulfide bonds within the protein (*21*). Formation or lack of the disulfide bonds may alter the activity of proteins.

Binding of Homogeneous XPA to DNA Substrates. The activity and specificity of the purified XPA were examined by gel mobility shift assays. As shown in Figure 2A, we observed two well-resolved XPA−DNA complexes with a

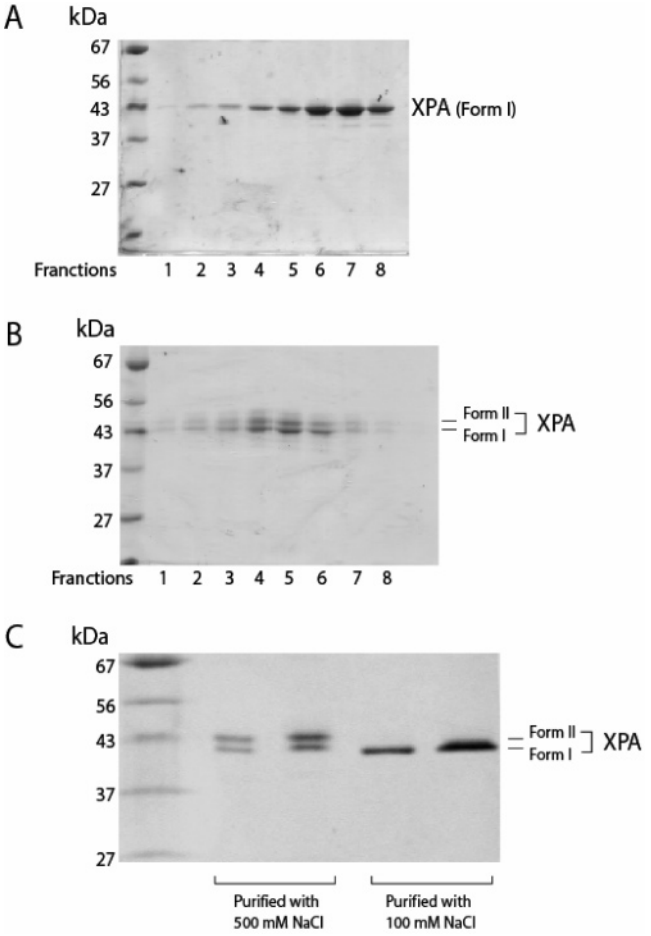

FIGURE 1: SDS−PAGE of purified XPA. $[His]_6$-XPA expressed from the sf21 cells was purified either with 100 mM (A) or 500 mM (B) (see Materials and Methods) and analyzed on an 8% SDS−PAGE stained with Coomassie Blue. (C) The comparison of the XPAs purified from different experimental conditions.

defined DNA substrate containing a site-specific single C8 guanine−AAF adduct, and formation of the specific complexes was clearly dependent on the concentration of XPA. At 100 nM, the XPA protein bound to the AAF-50-bp substrate and the protein−DNA complex appeared as a retardation band (the first shift) on the gel. However, when the concentration was increased to 300 nM or higher, a second band shift resulted with the loss of the first one. The average apparent overall $K_{d,ave}$ for the total binding was estimated to be about 200 nM. Upon increase of the XPA concentration up to 1.5 μM, the second shift remained unaffected, and no further shift was observed (data not shown). The same specific binding pattern was also observed with other types of DNA adducts (data not shown). However, the XPA showed little, if any, affinity for undamaged DNA, indicating that the XPA binds specifically to the damaged DNA but not to nondamaged DNA. Our results suggested that the first gel-shift represented the binding of an XPA to adduct, while the second shift was due to the interaction of an additional XPA to the XPA-coated DNA adduct or of an XPA dimer to the DNA substrate. A comparison in DNA binding was also made between the XPA proteins purified with the buffers containing 100 and 500 mM NaCl, respectively (Figure 2B). In the case of 500 mM salt, XPA failed to produce the first shift and the binding was less efficient than that with the protein purified with 100 mM NaCl.

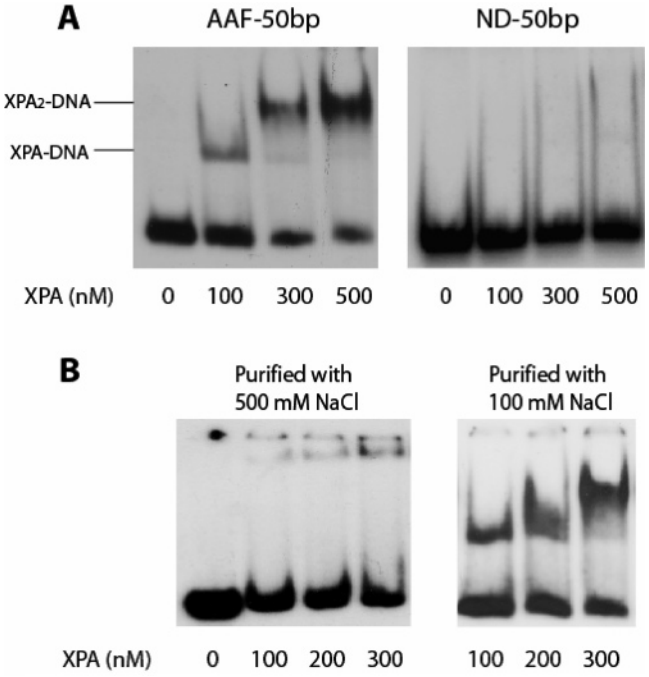

FIGURE 2: Interactions of XPA with AAF−DNA substrate. (A) XPA binds to a 50-bp AAF adduct showing two well-resolved XPA−DNA bands. The XPA of varying concentrations were incubated with AAF-50-bp or nondamaged (ND) substrate (2 nM) at 30 °C for 20 min in 20 μL binding buffer (20 mM Hepes, pH 7.9, 75 mM KCl, 5 mM $MgCl_2$, 1 mM EDTA, 1 mM DTT, 5% glycerol, and 100 mg/mL BSA). The mixtures were loaded onto a 3.5% native polyacrylamide gel and electrophoresed at 4 °C. (B) The same gel mobility shift assays for the binding of XPA purified with 100 mM and 500 mM NaCl to AAF-50-bp substrate, respectively.

Gel Filtration and Scintillation Analysis. The concentration dependency of XPA interaction with the AAF−DNA adduct was further investigated using the methods of gel filtration chromatography and liquid scintillation (Figure 3). In these experiments, the XPAs with concentrations from low to high were incubated with the AAF-50-bp substrate (5′ terminally labeled with ^{32}P), respectively, and then gel-filtrated on a Superdex-200 HR chromatography column driven by an AKTApurifier system (Amersham Pharmacia Biotech) under the DNA binding conditions. The fractions collected from the sizing column separation were then subjected to scintillation-counting for radioactivity (Figure 3A). Consistent with the results from gel mobility shift assays above, two major species with different retention volumes (RT) were identified, one with low XPA concentration (100 nM) and the other with protein concentration of 500 nM or higher. The data were further analyzed for molecular weight estimation using a broad range of molecular markers (Amersham Pharmacia Biotech) gel-filtrated under the same experimental conditions (Figure 3B). At 100 nM of XPA, the peak of the radioactivity count had a retention volume corresponding to a molecular weight (MW) of 65 kDa, suggesting that XPA bound to the substrate in the form of a monomer (MW_{XPA} = 36 kD, MW_{DNA} = 31 kD), whereas at the higher concentrations, the retention volume indicated a molecular weight of 98 kDa, which approximates that of a XPA dimer−DNA complex.

UV-Cross-Linking of DNA-Bound XPA. To further verify the complex formation of XPA dimer with DNA substrate, UV-cross-link assays were performed to cross-link the binding XPA protein to DNA. In this experiment, samples

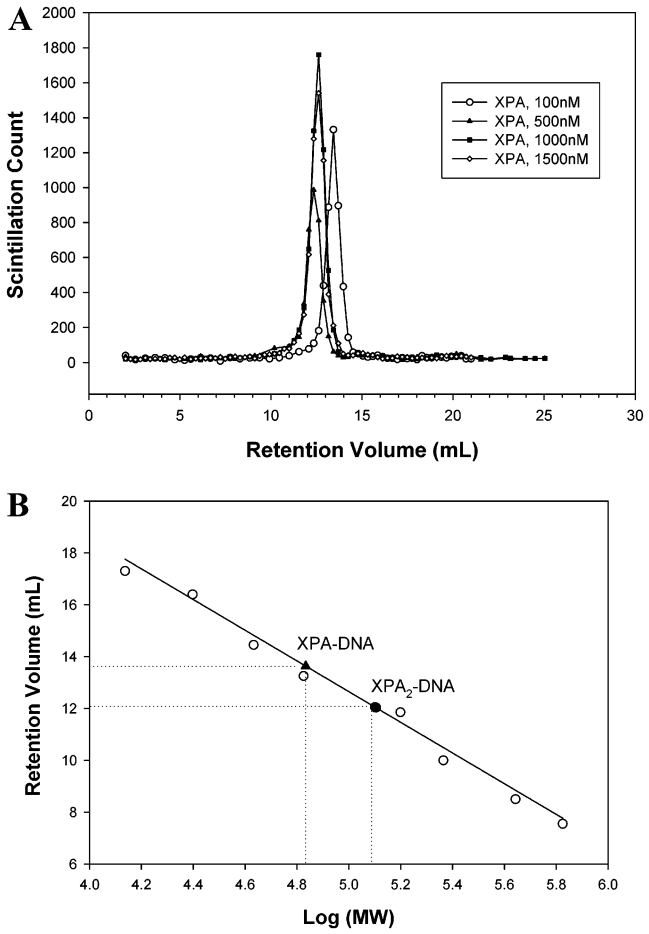

FIGURE 3: Gel filtration analysis of XPA binding to AAF-50-bp. (A) XPA protein at various concentrations (100−1500 nM) was incubated with 4 nM 5′ terminally [^{32}P]-labeled AAF-50-bp DNA substrate at 30 °C for 20 min in DNA binding buffer (20 mM Hepes, pH 7.9, 75 mM KCl, 5 mM $MgCl_2$, 1 mM EDTA, 1 mM DTT, 5% glycerol, and 100 mg/mL BSA). The mixture was then loaded onto a Superdex-200 HR column running with binding buffer for separation. Fractions (200 μL) were collected and counted for radioactivity. The radioactive intensities of fractions were plotted against the corresponding retention volume. (B) The molecular weights of the formed XPA−DNA complexes were determined based on a set of molecular mass markers (ribonuclease A, 13.7 kDa; chymotrysinogen A, 25 kDa; ovalbumin, 43 kDa; albumin, 67 kDa; aldolase, 158 kDa; catalase, 232 kDa; ferritin, 440 kDa; and thyrog-lobulin, 669 kDa) and gel-filtrated under the same condition as the XPA samples. Data for these markers were fitted with linear regression method. At 100 nM of XPA, the retention volume corresponds to a molecular weight of 65 kDa, while at the concentrations ≥500 nM, the retention volume of XPA−DNA complex indicates a molecular weight of 98 kDa.

of XPA−DNA interaction under the same conditions as in the gel mobility shift assays described above were UV-irradiated at 245 or 312 nm, followed by analysis on SDS−PAGE. As shown in Figure 4A, the UV irradiation resulted in the formation of a radioactive protein−DNA cross-linking product of about 84 kDa at the XPA concentration of 500 nM. This strongly suggests that an XPA dimer was cross-linked to the DNA. A similar experiment was also performed for analysis by Western blotting with XPA antibody (Figure 4B). Consistently, a cross-link product of XPA_2−DNA was obtained. The cross-linking was specific and depended on the presence of DNA substrate, as the same concentration of XPA in the absence of DNA resulted in little, if any, cross-link product (Figure 4B, lane 1).

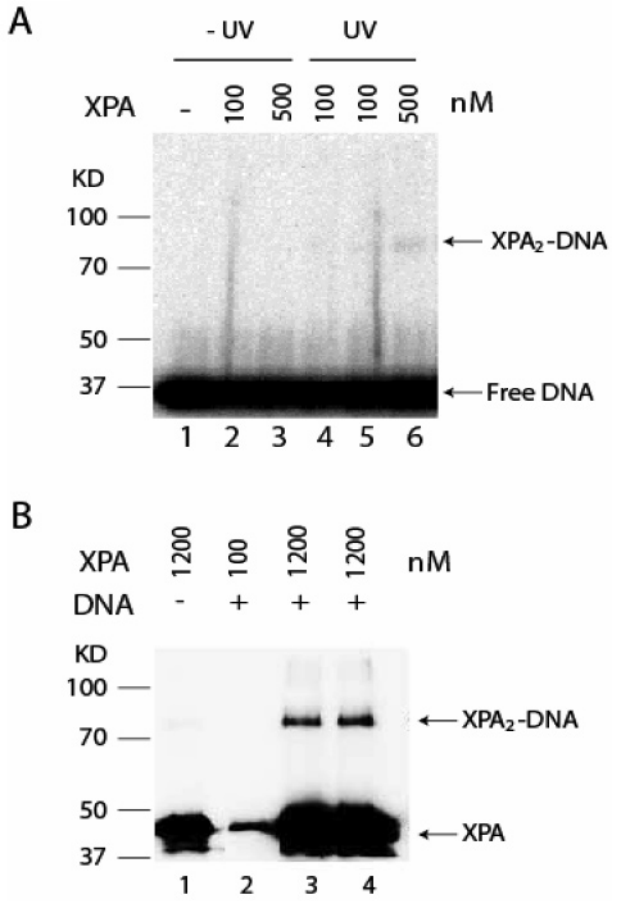

FIGURE 4: Cross-linking of XPA−DNA complex by UV irradiation. (A) ^{32}P terminally labeled AAF−DNA substrate was incubated with the indicated concentrations of XPA and then subjected to UV irradiation (254 nm) at 14 J m^{-2} s^{-1}. The samples were analyzed on 8% SDS−PAGE. The radioactivity of the gel was detected by phosphorimage scanner. (B) The samples were prepared as the same as in panel A except that the UV irradiation was performed at 312 nm. After 8% SDS−PAGE separation, the gel was subjected to Western blotting with anti-XPA antibody.

Competitive Binding Analysis. To further examine the formation of the two complexes of different gel mobility shifts, the specific binding of the XPA to AAF-50-bp adduct was challenged by nonradioactive and nondamaged 50-bp DNA in a competitive binding assay. As shown in Figure 5, at 100 nM of XPA which formed a complex with the adduct as the first band shift, the presence of the nondamaged DNA did compete gradually, albeit not very efficiently, with the specific binding, as the molar ratio of the nondamaged to damaged DNA increased from 0 to 200. In comparison, for the XPA at 500 nM, no significant competition from the nondamaged DNA was observed for the specific binding of XPA to adduct (the second shift) even as the molar ratio of nondamaged to damaged DNA increased to 200. This result indicated that binding of the second XPA to the XPA-bound DNA adduct stabilized the DNA damage recognition of XPA. The involvement of the second XPA in the binding enhanced the specific binding of XPA to the adduct, indicating a positive cooperative interaction.

To quantitatively assess the positively cooperative binding of the XPA to the damaged DNA, fluorescence anisotropy measurement was conducted. In this experiment, the AAF-50-bp DNA substrate with a 5′ terminally labeled fluorescein was titrated with varying concentrations of XPA. As shown

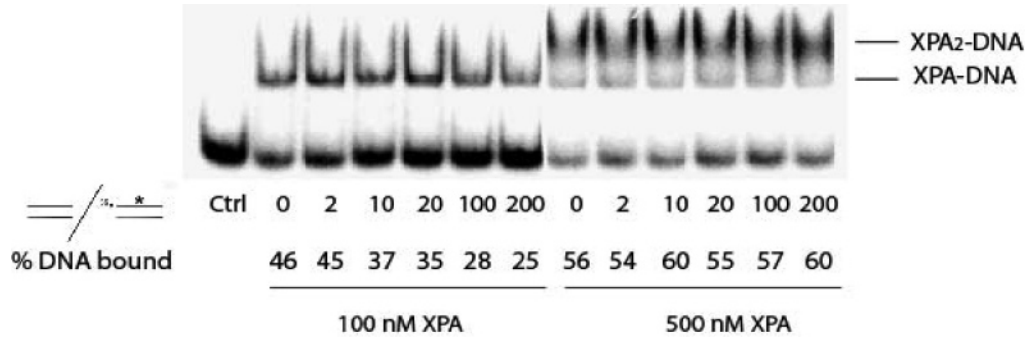

FIGURE 5: Competitive binding of nondamaged and damaged DNA to XPA. The XPA protein (100 nM and 500 nM) was incubated with [^{32}P]-labeled AAF-50-bp DNA substrate at 30 °C for 20 min in the binding buffer in the presence of nondamaged 50-bp DNA (nonradioactive) at various concentrations or ratios of nondamaged DNA to damaged DNA. Samples were then analyzed by gel mobility shift assays at 4 °C. The XPA−DNA complex formation was quantified as the percentage of DNA bound to XPA.

in Figure 6A, the binding isotherm displayed a sigmoid characteristic. Nonlinear least-squares fitting of these titration data gave the binding constants of $K_1 = 1.4 \times 10^6$ M^{-1} and $K_2 = 1.8 \times 10^7$ M^{-1}, for the first and second bindings of XPA to DNA, respectively. This indicates that the second XPA binding, which was about 12-fold more efficient than the first one, exhibited a high positive cooperativity with the initial XPA binding. Figure 6B shows the Hill plot of the titration data. From this plot, a Hill coefficient of 1.9, the slope at $\log(\theta) = 0$, was obtained, indicating a positively cooperative interaction of XPA with DNA substrate.

Interaction of RPA and XPA with DNA Adduct. Since the interaction of XPA with RPA has been suggested to play an important role in nucleotide excision repair, we investigated the effects of RPA on the specific binding of XPA to the AAF adduct. For the XPA at 100 nM, the presence of RPA resulted in no considerable increase in overall binding of the proteins to the DNA adduct (Figure 7, lanes 2−4, 6, and 7). Similar results were also obtained in the presence of the higher XPA concentration (500 nM) (Figure 7, lanes 5, 8, and 9), even though in this case, most of the XPA−DNA complexes were converted to the XPA$_2$−RPA−DNA complex (comparison between lanes 5 and 8 or 9). In sum, the data in Figure 7 do not support a significant cooperative binding of RPA and XPA to AAF-adducted DNA.

DISCUSSION

Determination of the molecular mechanism of XPA in human NER depends on our understanding of the biochemical interaction of XPA with DNA damage. In the present study, using a purified homogeneous form of XPA, we have studied the stoichiometric binding of XPA to a C8 guanine adduct of AAF and also demonstrated that the damage recognition of XPA is a stepwise process facilitated by the positively cooperative interactions of XPA molecules with DNA adduct.

Our results showed that, while a DNA lesion was recognized by a single XPA protein molecule, the more stable form of the specific binding complex involved the interaction of two XPA molecules with the DNA lesion. It should be noted that the length of the 50-bp DNA substrate containing a single AAF adduct used in this study was long enough for multiple XPA molecules to bind nonspecifically (if this occurs) as the protein has a Stokes radius of 33 Å (*14*). Thus, upon binding of the first XPA to the single adduct site, the second XPA may bind either independently to the nondam-

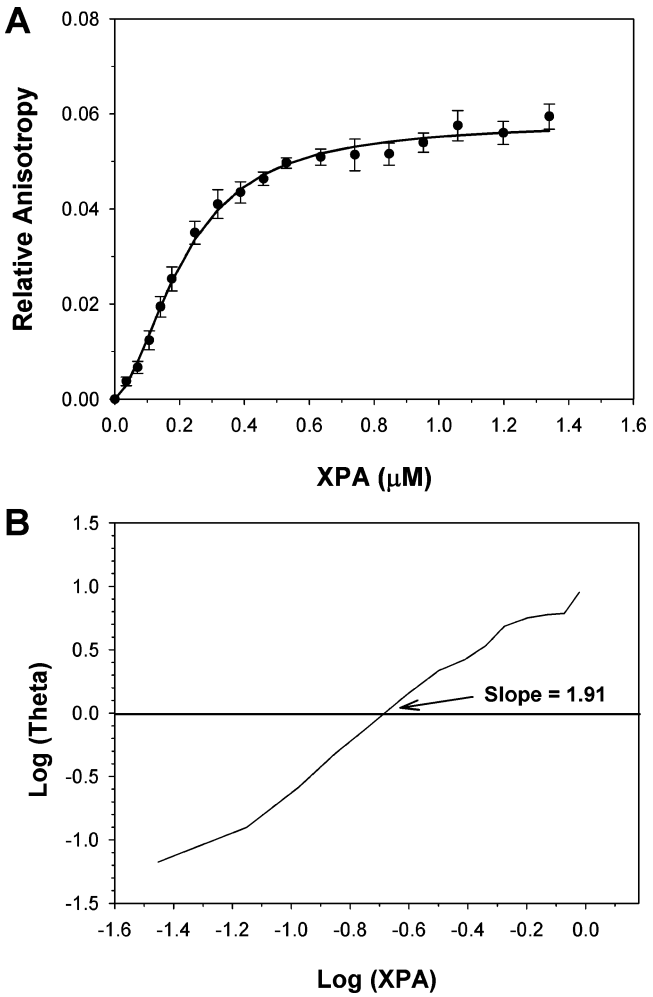

FIGURE 6: Fluorescence anisotropy measurements of XPA binding to 5′F-AAF-50-bp. (A) Binding isotherm was generated by titrating the 5′ terminally labeled AAF-50-bp DNA (10 nM) with XPA protein in 200 μL of binding buffer. The anisotropy was recorded at an emission wavelength of 520 nm with an excitation wavelength of 492 nm. The anisotropy data was normalized by subtracting the initial value of free DNA. The error bars indicate the standard deviation of at least three independent experiments. The solid line represents the best fitting of the binding isotherm with a two-binding model by nonlinear least-squares strategy as described in Materials and Methods. From the fitting, the binding constants were determined as $K_1 = 1.4 \times 10^6$ M^{-1} and $K_2 = 1.8 \times 10^7$ M^{-1}. (B) The fluorescence anisotropy data were analyzed by Hill plot, which gave a Hill coefficient of 1.91, an indication of possible cooperative interaction of XPA with DNA adduct.

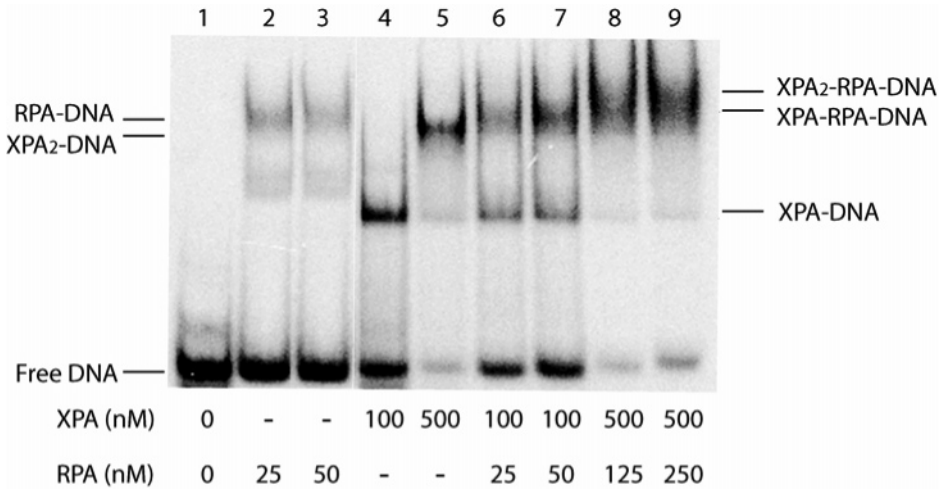

FIGURE 7: Interaction of RPA and XPA with AAF−DNA substrate. The XPA at 100 and 500 nM were incubated with AAF-50-bp DNA in the presence (lanes 6−9) and absence (lane 4−5) of RPA of various concentrations at 30 °C for 20 min in binding buffer. Samples were analyzed by gel mobility shift assays on a 3.5% native polyacrylamide gel at 4 °C. Lanes 2−3, RPA binds to the DNA substrate in the absence of XPA.

aged and unbound region of the DNA or cooperatively to the XPA-bound DNA adduct. Our results suggest that the latter is likely true, based on the data from our competition assay (Figure 5) and the observation that the XPA had little, if any, affinity for unadducted DNA. More importantly, the nonspecific binding does not increase the stability of the XPA−DNA complex formation. We propose that the adduct (or perhaps the local distortion in DNA due to the presence of the adduct) was initially recognized by an XPA protein, forming a protein−adduct complex with a structure energetically favorable for an additional XPA molecule to bind. The binding of the second XPA resulted in the formation of a much more stable recognition complex. The increase in binding affinity of XPA to the DNA adduct by at least an order of magnitude as exhibited by the step binding constants of K_1 and K_2, indicated that the XPA dimer had a much higher affinity for the adduct than the monomer, but formation of the XPA dimer−DNA complex depends on the monomeric XPA−DNA interaction in a sequential cooperative binding. In a different possible scenario, an XPA monomer may exist as a dominant form at low concentration of XPA, while an XPA dimer may prevail at high concentration of the protein. Thus, at low concentration of XPA, only the XPA monomer−DNA complex was observed, and at high concentration, the major complex formation is XPA dimer−DNA interaction. Although both XPA monomer and dimer bind to the DNA adduct, the dimer appeared to have a much higher affinity to DNA lesion.

No matter which scenario is true, the DNA damage recognition by an XPA dimer or monomer depends on the concentration of the protein. Thus, it would be of great interest to determine if the concentration of XPA plays a role in regulation of XPA functions in cells via the concentration-dependent formation of different types of XPA-damaged DNA complexes. We have noticed that upon UV irradiation of human cells, XPA molecules extensively translocated from cytoplasm to nucleus, allowing the enrichment and considerable increase of the protein concentration in nucleus (data not shown). Also, it has been demonstrated that the cellular concentration of XPA has significant effects on the UV resistance of human cells, age-associated DNA repair capacity, and the cisplatin sensitivity in testis tumors (*22*−*24*).

Interestingly, our results also showed that the presence of RPA had no significant effects on the damage recognition of XPA. This is in agreement with a recent observation that loading of RPA onto DNA lesions was independent of XPA in cells (*12*). Also, it was recently suggested that XPA and RPA were recruited separately to the damaged site in the mechanism of NER (*13*). Despite these, interaction of XPA and RPA still may be crucial to the success of human nucleotide excision repair, such as stabilization of the RPA−DNA complex formation and inhibition of strand separation activity of RPA (*25*) and recruitment and assembly of NER factors (*1*). Evidently, more studies are needed to elucidate the details of the roles of XPA and RPA in NER.

REFERENCES

1. Petit, C., and Sancar, A. (1999) Nucleotide excision repair: from *E. coli* to man, *Biochimie 81*, 15−25.
2. Wood, R. D. (1999) DNA damage recognition during nucleotide excision repair in mammalian cells, *Biochimie 81*, 39−44.
3. Thoma, B. S., and Vasquez, K. M. (2003) Critical DNA damage recognition functions of XPC-hHR23B and XPA-RPA in nucleotide excision repair, *Mol. Carcinog.* 1−13.
4. Hanawalt, P. C. (1994) Transcription-coupled repair and human disease, *Science 266*, 1957−1958.
5. de Laat, W. L., Jaspers, N. G., and Hoeijmakers, J. H. (1999) Molecular mechanism of nucleotide excision repair, *Genes Dev. 13*, 768−785.
6. Li, L., Elledge, S. J. Peterson, C. A., Bales, E. S., and Legerski, R. J. (1994) Specific association between the human DNA repair proteins XPA and ERCC1, *Proc. Natl. Acad. Sci. U.S.A. 91*, 5012−5016.
7. Park, C. H., and Sancar, A. (1994) Formation of a ternary complex by human XPA, ERCC1, and ERCC4(XPF) excision repair proteins, *Proc. Natl. Acad. Sci. U.S.A. 91*, 5017−5021.
8. Nocentini, S., Coin, F., Saijo, M., Tanaka, K., and Egly, J.-M. (1997) DNA damage recognition by XPA protein promotes efficient recruitment of transcription factor II H, *J. Biol. Chem. 272*, 22991−22994.
9. Evans, E., Moggs, J. G., Hwang, J. R., Egly, J. M., and Wood, R. D. (1997) Mechanism of open complex and dual incision formation by human nucleotide excision repair factors, *EMBO J. 16*, 6559−6573.
10. Sugasawa, K., Ng, J. M., and Masutani, C. (1998) Xeroderma pigmentosum group C protein complex is the initiator of global genome nucleotide excision repair, *Mol. Cell 2*, 223−232.

11. Missura, M., Buterin, T., Hindges, R., Hubscher, U., Kasparkova, J., Brabec, V., and Naegeli, H. (2001) Double-check probing of DNA bending and unwinding by XPA-RPA: an architectural function in DNA repair, *EMBO J. 20*, 3554−3564.
12. Rademakers, S., Volker, M., Hoogstraten, D., Nigg, A. L., Mone, M. J., van Zeeland, A. A., Hoeijmakers, J. H. J., Houtsmuller, A. B., and Vermeulen, W. (2003) Xeroderma pigmentosum group A protein loads as a separate factor onto DNA lesions, *Mol. Cell Biol. 23*, 5755−5767.
13. Riedl, T., Hanaoka, F., and Egly, J.-M. (2003) The comings and goings of nucleotide excision repair factors on damaged DNA, *EMBO J. 22*, 5293−5303.
14. Jones, C. J., and Wood, R. D. (1993) Preferential binding of the xeroderma pigmentosum group A complementing protein to damaged DNA, *Biochemistry 32*, 12096−12104.
15. He, Z., Henricksen, L. A., Wold, M. S., and Ingles, C. J. (1995) RPA involvement in the damage-recognition and incision steps of nucleotide excision repair, *Nature 374*, 566−569.
16. Wakasugi, M., and Sancar, A. (1999) Order of assembly of human DNA repair excision nuclease, *J. Biol. Chem. 274*, 18759−18768.
17. Hermanson, I. L., and Turchi, J. J. (2000) Overexpression and purification of human XPA using a baculovirus expression system, *Protein Expression Purif. 19*, 1−11.
18. Yang, Z., Liu, Y., Mao, L. Y., Zhang, J.-T., and Zou, Y. (2002) Dimerization of human XPA and formation of XPA_2−RPA protein complex, *Biochemistry 41*, 13012−13020.
19. Luo, C., Krishnasamy, R., Basu, A., and Zou, Y. (2000) Recognition and incision of site-specifically modified C8 guanine adducts formed by 2-aminofluorene, *N*-acetyl-2-aminofluorene and 1-nitropyrene by UvrABC nuclease, *Nucleic Acids Res. 28*, 3719−3724.
20. Dahlquist, F. W. (1978) The meaning of Scatchard and Hill plots, *Methods Enzymol. 48*, 270−299.
21. Iakoucheva, L. M., Kimzey, A. L., Masselon, C. D., Smith, R. D., Dunker, A. K., and Ackerman, E. J. (2001) Aberrant mobility phenomena of the DNA repair protein XPA, *Protein Sci. 10*, 1353−1362.
22. Cleaver, J. E., Charles, W. C., McDowell, M. L., Sadinski, W. J., and Mitchell, D. L. (1995) Overexpression of the *xpa* repair gene increases resistance to ultraviolet radiation in human cells by selective repair of DNA damage, *Cancer Res. 55*, 6152−6160.
23. Koberle, B., Masters, J. R. W., Hartley, A. A., and Wood, R. D. (1999) Defective repair of cisplatin-induced DNA damage caused by reduced XPA protein in testicular germ cells tumors, *Curr. Biol. 9*, 273−276.
24. Goukassian, D., Gad, F., Yaar, M., Eller, M. S., Nehal, U. S., and Gilcherest, B. A. (2000) Mechanisms and implications of the age-associated decrease in DNA repair capacity, *FASEB J. 14*, 1325−1334.
25. Patrick, S. M., and Turchi, J. J. (2002) Xeroderma pigmentosum complementation group A protein (XPA) modulates RPA-DNA interactions via enhanced complex stability and inhibition of strand separation activity, *J. Biol. Chem. 277*, 16096−16101.

BI047598Y